Bioscience of Microbiota, Food and Health Vol. 43 (1), 43–54, 2024

Full Paper

Effects of food-grade iron(III) oxide nanoparticles on cecal digesta- and mucosa-associated microbiota and short-chain fatty acids in rats

Jiangchun SHI[1], Yumeng XIE[1], Yulin LI[2], Dongxia REN[3], Yiqi ZHANG[1], Huangfang SHAO[1], Yang LIU[1], Xue WANG[1] and Yun LI[1, 4*]

[1]*West China School of Public Health and West China Fourth Hospital, Sichuan University, Chengdu 610041, China*
[2]*Department of Hospital-acquired Infection Management, Guizhou Provincial People's Hospital, Guiyang 550002, China*
[3]*Department of Blood Transfusion, Tangdu Hospital, Fourth Military Medical University, Xi'an 710032, China*
[4]*Provincial Key Laboratory of Food Safety Monitoring and Risk Assessment of Sichuan, Chengdu 610041, China*

Received February 15, 2023; Accepted August 21, 2023; Published online in J-STAGE September 12, 2023

Although iron(III) oxide nanoparticles (IONPs) are widely used in diverse applications ranging from food to biomedicine, the effects of IONPs on different locations of gut microbiota and short-chain fatty acids (SCFAs) are unclear. So, a subacute repeated oral toxicity study on Sprague Dawley (SD) rats was performed, administering low (50 mg/kg·bw), medium (100 mg/kg·bw), and high (200 mg/kg·bw) doses of IONPs. In this study, we found that a high dose of IONPs increased animal weight, and 16S rRNA sequencing revealed that IONPs caused intestinal flora disorders in both the cecal digesta- and mucosa-associated microbiota. However, only high-dose IONP exposure changed the abundance and composition of the mucosa-associated microbiota. IONPs increased the relative abundances of *Firmicutes*, *Ruminococcaceae_UCG-014*, *Ruminiclostridium_9*, *Romboutsia,* and *Bilophila* and decreased the relative abundance of *Bifidobacterium,* and many of these microorganisms are associated with weight gain, obesity, inflammation, diabetes, and mucosal damage. Functional analysis showed that changes in the gut microbiota induced by a high dose of IONPs were mainly related to metabolism, infection, immune, and endocrine disease functions. IONPs significantly elevated the levels of valeric, isobutyric, and isovaleric acid, promoting the absorption of iron. This is the first description of intestinal microbiota dysbiosis in SD rats caused by IONPs, and the effects and mechanisms of action of IONPs on intestinal and host health need to be further studied and confirmed.

Key words: iron oxide nanoparticles, digesta-associated microbiota, mucosa-associated microbiota, short-chain fatty acids

INTRODUCTION

With the rapid development of nanotechnology in the last decade, iron(III) oxide nanoparticles (IONPs) have become widely used in food, medicine, construction, paints/coating, plastics, and other applications [1]. They are also frequently present in high quantities in food pigments used in chewing gums, edible ices, cheeses, flavored drinks, food supplements, and other products. Furthermore, along with the increasing opportunities for much broader public exposure of the human body to IONPs, more attention is being given to their potential risk to human health. In 1980, an acceptable daily intake of 0–0.5 mg/kg·body weight (bw)/day was established by the Joint FAO/WHO Expert Committee of Food Additives (JECFA). In the US, IONPs can only be used for the coloring of sausage casings, and their amounts are limited to 0.10% of the overall food weight [2].

To date, the toxic effects of IONPs have not been systematically established, as research on this subject is scarce, required data are unavailable, and past results have been contradictory. It is well known that the iron released from IONPs can contribute to Fenton's reaction, generating reactive oxygen species (ROS) from H_2O_2 and superoxide, which causes oxidative stress and ultimately damages cells [3]. Some studies have shown that IONPs can induce cytotoxicity, genotoxicity, developmental toxicity, neurotoxicity, immunotoxicity, and other toxic effects [4, 5]. Subacute or subchronic oral IONP exposure resulted in

*Corresponding author. Yun Li (E-mail: liyun_611@163.com)
(Supplementary materials: refer to PMC https://www.ncbi.nlm.nih.gov/pmc/journals/2480/)

doi: 10.12938/bmfh.2023-012

varying degrees of negative effects in Sprague Dawley (SD) rats in our previous studies of absorption, distribution, metabolism, and excretion (ADME), including accumulation in various organs and tissues; elevated serum, tissue, urine, and fecal iron and oxidative stress levels [6, 7]; and the potential to increase fasting blood glucose levels and impair rat liver lipid metabolism [8]. In fact, consumers are more frequently exposed to foods containing nanoparticles (NPs) than most people think, and when these NPs enter the gastrointestinal tract (GIT) through food intake, one of the concerns surrounding them is their potential to induce changes in the microbiome [9]. Silver, titanium dioxide (TiO_2), and zinc NPs have been found to have adverse effects on gut microbiota [10, 11]. Most published studies have discussed that iron and iron oxide nanoparticles are more widely used for iron deficiency than traditional iron-based supplement treatments and indicated that they are nontoxic and do not change the gut microbiota, even promoting beneficial microbiota [9, 12]. In addition, it has been discussed that IONPs can generate toxic ROS and affect commensal microbes, such as *Escherichia coli*, *Staphylococcus aureus*, and *Bacillus subtilis* [13]. However, Medina-Reyes *et al.* [14] indicated that no studies have evaluated gut microbial alterations caused by IONPs or E172 after oral exposure. All of these findings aroused our interest in the effects of IONPs on gut microbiota.

The gut microbiota has coevolved with its host and is involved in digestion, nutrient extraction, energy supply, immune modulation, prevention of intestinal pathogens, and other processes and functions [15]. Disruption of the normal balance between the gut microbiota and the host may cause some gastrointestinal diseases, including colorectal cancer (CRC) [16] and inflammatory bowel disease (IBD) [17], and even the development of noninfectious chronic metabolic diseases, such as obesity [18], type 2 diabetes [19], nonalcoholic liver disease, cardiometabolic diseases, and malnutrition [20]. The major products from the microbial fermentation of fiber and resistant starch via colonic anaerobic bacteria in the gut are short-chain fatty acids (SCFAs), especially acetic, propionic, and butyric acids. SCFAs are present at the highest levels in the cecum and proximal colon (70–140 mM), while their concentrations decrease toward the distal colon (20–70 mM) and distal ileum (20–40 mM) [21]. SCFAs play an important role in maintaining gut and immune homeostasis and have been shown to have anti-inflammatory, antitumorigenic, and antimicrobial properties and to alter gut integrity [18].

Changes in diet can rapidly affect the composition of gut microbiota and in turn the relative amounts of the different SCFAs produced, eventually affecting human health. Presently, studies on gut microbiota have mainly been performed with samples collected from feces and intestinal content, while studies on changes in mucosal microbiota are lacking; in proximity to the epithelium, microbes present within the mucosa exert a greater effect on the host than digesta microbes [22]. Substantial differences between the digesta- and mucosa-associated gut microbiota have been revealed [23], and digesta- and mucosa-associated gut microbiota may respond differently to dietary changes. However, how IONPs may influence intestinal health, function, and microbiota and the production of SCFAs remains largely unexplored, and it is important to assess any possible hazards of IONPs associated with ingestion. As far as we know, we are the first to identify the potential hazards of IONPs in relation to the gut microbiota and SCFAs and explored the responses of different locations of the intestine to IONPs, and this study provides important insight concerning assessment of the impacts of IONPs on gut microbiota.

MATERIALS AND METHODS

Chemicals and reagents

Origin and characteristics of the IONPs

The IONPs used in this study were purchased from Shanghai Supermicro Nano Technology. Co. Ltd. (Shanghai, China); they were reddish brown and 99.9% pure. The purchased IONPs were characterized with respect to particle size, hydrodynamic size, and surface properties in a previous study [8]. After being analyzed by transmission electron microscopy (TEM; Tecnai F30, FEI Company, Hillsboro, OR, USA), the IONPs were determined to be rod-shaped, and the particle size was mainly distributed at 70 ± 10 nm. Dynamic light scattering (DLS) measurements showed that the hydrodynamic size of IONPs was approximately 176.8 ± 11 nm. The surface potential of the IONPs, as measured by zeta potential (Zetasizer Nano ZS, Malvern Panalytical, Malvern, UK), was +25 mV at pH 7.

Other chemicals and reagents

Hydroxypropyl methylcellulose (HPMC) was purchased from Shanghai Yuanye Biological Technology. Co. Ltd. (Shanghai, China). A DNeasy PowerSoil Kit and QIAamp 96 PowerFecal QIAcube HT Kit were purchased from QIAGEN (Hilden, Germany). A Qubit dsDNA Assay Kit was purchased from Thermo Fisher Scientific (Waltham, MA, USA). Takara Ex Taq was purchased from Takara (Kusatsu, Japan). HPLC-grade SCFA standards were purchased from MilliporeSigma (Burlington, MA, USA). HPLC-grade pyridine, propanol, and hexane were purchased from CNW (Munich, Germany). Analysis-grade NaOH and Na_2SO_4 were purchased from Sinopharm (China National Pharmaceutical Group Corporation, Beijing, China). Physiological saline was purchased from Sichuan Kelun Industry Group Co. Ltd. (Sichuan, China).

Subacute repeated oral toxicity study

Animal study design

Five-week-old male SD rats were obtained from Beijing Vital River Laboratory Animal Technology Co., Ltd. (SCXK 2016-0011) and kept at 22 ± 2°C and 50 ± 10% relative humidity with a light-dark cycle of 12 hr. After 5 days of adaptive feeding, six rats were assigned to each of the control group (group C, 0.5% HMPC solution) and 3 different IONP-treated groups, the low-dose (group L, 50 mg/kg·bw), middle-dose (group M, 100 mg/kg·bw), and high-dose groups (group H, 200 mg/kg·bw), by a body weight stratification and randomization method. The experimental doses were based on the oral intake dose for E172 estimated by the JECFA in 1980 with a 100-fold uncertainty factor [2]. Oral administration was performed once a day for 28 consecutive days, and the dosage was adjusted according to

weekly weighing results. All animal experiments followed the guidance of the Ethical Committee for Research on Laboratory Animals of Sichuan University.

General observations and hematological and biochemical analyses

All rats were observed for changes in skin, eyes, posture, ingestion, behaviors, bowel movement, morbidity, and mortality. Body weights were measured and recorded on test days 0, 3, 7, 14, 21, and 28. At the end of the experiment, surviving animals were fasted overnight for 12 hr. Before necropsy, all animals were weighed and anesthetized by intraperitoneal administration of 10% chloral hydrate. Then, whole blood was collected into both ethylene diamine tetraacetic acid (EDTA)-containing and nonheparinized tubes for hematological and biochemical analyses.

Histological analyses

After the blood samples were collected, the liver, kidneys, brain, lungs, heart, spleen, and thymus were excised and weighed. The cecum was separated, fixed in 4% formalin for 48 hr, embedded in paraffin, and sectioned with a rotary microtome (MICROM International GmbH, Hessen, Germany). Random tissue sections (5 µm) of the cecum were stained with hematoxylin and eosin (HE) and observed with an optical microscope (BA210 Digital, Motic, Fujian, China). Prussian blue staining was used to observe iron accumulation in cecal tissue. The above tissue was stained using 10% potassium ferrocyanide and 20% hydrochloric acid for 20 min. Iron staining was observed with an optical microscope (BA210 Digital, Motic, Fujian, China).

16S rRNA sequencing and data analysis

The cecal intestinal segment was cut, and the digesta were extruded with sterile forceps and transferred to a sterile cryopreservation tube. The segment was then rinsed in phosphate-buffered saline (PBS) three times to remove remnants of the digesta for investigation of the mucosa-associated bacteria collected by scraping the mucosal layer from two centimeters of the cecal segment with a sterile scalpel. The samples were stored at −80°C until the assay and ultimately ground for the subsequent analysis. Total cecal digesta and cecal mucosal DNAs were extracted using a DNeasy PowerSoil kit (QIAGEN) according to the manufacturer's instructions. DNA concentration and quality were tested using a NanoDrop 2000 spectrophotometer (Thermo Fisher Scientific, Waltham, MA, USA) and 1% agarose gel electrophoresis, respectively. The V3–V4 regions of the 16S rRNA genes were amplified by specific primer pairs (343F, 798R). The first PCR program included 5 min at 94°C; 26 cycles of 30 sec at 94°C, 30 sec at 56°C, and 72°C for 20 sec; and then 5 min at 72°C. The second PCR program included the same conditions as the first PCR but with only 7 cycles. The amplicon products were purified with Agencourt AMPure XP beads (Beckman Coulter Genomics, Brea, CA, USA). The purified PCR products were verified to be single bands by gel extraction with a QIAGEN gel extraction kit (QIAGEN). The concentration and length distribution of the DNA library were tested with a Qubit Fluorometer (Invitrogen, Carlsbad, CA, USA).

The Illumina MiSeq PE300 platform (Illumina Inc., San Diego, CA, USA) was used to obtain raw sequencing data in fastq format. The paired-end reads were de-hybridized using the Trimmomatic software [24]. Also, QIIME was used to detect reads (containing N bases, single base repeats greater than 8, lengths less than 200 bp), and UCHIME was used to remove the chimeric sequences from the sequences [25]. Then, sequences were grouped into operational taxonomic units (OTUs) based on sequence similarity using the Vsearch software [26], and sequences with sequence similarity parameters greater than or equal to 97% were grouped into one OTU unit. Representative sequences for each OTU were selected using the QIIME package [25] and annotated using the Silva database and the RDP classifier software [27], and confidence intervals greater than 0.7 were retained. Principal coordinate analysis (PCoA) was conducted with R based on weighted UniFrac distances. A linear discriminant analysis (LDA) coupled with effect size measurement (LefSe) analysis, also called a biomarker analysis, was used to explore the biomarkers in each group. A functional prediction analysis was also performed using the PICRUSt2 software.

Determination of SCFA concentrations

Fresh feces of SD rats were collected on days 1, 7, 14, and 28 of intragastric administration and quickly stored in a refrigerator at −80°C. The standard stock solution was obtained by dissolving an appropriate proportion of standards with deionized water using an analytical balance (SQP Practum213-1CN, Sartorius, Goettingen, Germany), and the concentration of the stock solution was 1 mg/mL. Then, the stock solution was prepared as a mixed standard solution, which was diluted in a gradient with concentrations of 0.5 µg/mL, 1 µg/mL, 2 µg/mL, 5 µg/mL, 10 µg/mL, 20 µg/mL, 50 µg/mL, and 100 µg/mL, and standard curves were plotted according to the relative peak areas (peak areas of the standards/peak areas of the internal standards) at different concentrations and corresponding concentrations. Next, 100 mg of rat feces were added to 2 mL NaOH solution (5 mM), extracted ultrasonically for 7 min, and then centrifuged (12,000 rpm) at 4°C for 10 min. Then, 1,000 µL supernatant was removed by adding 200 µL propanol, 133 µL pyridine, and 67 µL propyl chloroformate and then vortexing for 10 sec. This was followed by the addition of 800 µL hexane and vortexing for 10 sec, centrifugation (12,000 rpm) at 4°C for 10 min, removal of 600 µL supernatant, and then extraction again with hexane. The substances in samples were detected by GC-MS (QP2010 Plus, Shimadzu, Kyoto, Japan), and their contents were calculated based on the plotted standard curves and the peak areas of the substances in the samples tested.

Statistical analysis

All data are presented as the mean ± standard error of the mean (SEM). If data followed a normal distribution and the variances were homogeneous, one-way ANOVA was performed for comparisons among the four groups, and the t-test was used for comparisons between two groups. Otherwise, the non-parametric Kruskal–Wallis H-test was applied for comparisons among the four groups, indicators with significant differences were subjected to the two-by-two comparison approach with Bonferroni correction, and the Mann–Whitney U test was used to identify the groups that were significantly different from the control group. The Wilcoxon rank-sum test was used in the LEfSe analyses to detect significantly different abundances in specific taxa among groups. Correlation coefficients between gut microbiota and the levels of SCFAs were calculated via Spearman's correlation

doi: 10.12938/bmfh.2023-012

analysis. The data were analyzed using the IBM SPSS Statistics 26 software (IBM Corp., Armonk, NY, USA). $P<0.05$ was considered statistically significant.

RESULTS

Subacute repeated oral toxicity study

Body weight, organ weight, and hematological and biochemical results

There were no mortalities in any of the dosage groups (groups C, L, M, and H) during the study period. The rats in all the groups continued to gain weight normally throughout the subacute oral toxicity study (Supplementary Fig. 1), and the weights of the L, M, and H dosage groups were higher than that of group C, especially the high-dose group after day 7. The organ to body weight ratios (%) of the brain and thymus in the high-dose group were significantly different from those of group C (Supplementary Table 1), but there were no significant differences in the organ to body weight ratios of the other groups (Supplementary Table 1). There were scarce changes in the hematological and biochemical parameters of the dosage groups, and they were small (Supplementary Tables 2 and 3), indicating that the differences were not adverse effects of the IONP treatments.

Assessment of cecal injury

The pathological changes induced by IONPs in the cecal tissues of the rats in each dosage group are shown in Fig. 1A. No obvious pathological changes were found. The cecal structure was intact in every treatment group, with visible stratification of the mucosal, submucosal, and muscle layers and outer membrane. In the IONP-treated groups, different degrees of blue particles were deposited in the intestinal cavity. Moreover, in groups M and H, blue particles accumulated in the loose connective tissue between the intestinal glands of the lamina propria, and the accumulation was larger in group H. However, no evident deposition of blue particles was discovered in Group C (Fig. 1B).

Effects of IONPs on gut microbiota

Effects of IONPs on the α- and β-diversity of gut microbiota

Microbiota diversity and the compositions of the cecal digesta and cecal mucosa of the control and IONP-treated groups were investigated by 16S rRNA sequencing. There were a total of

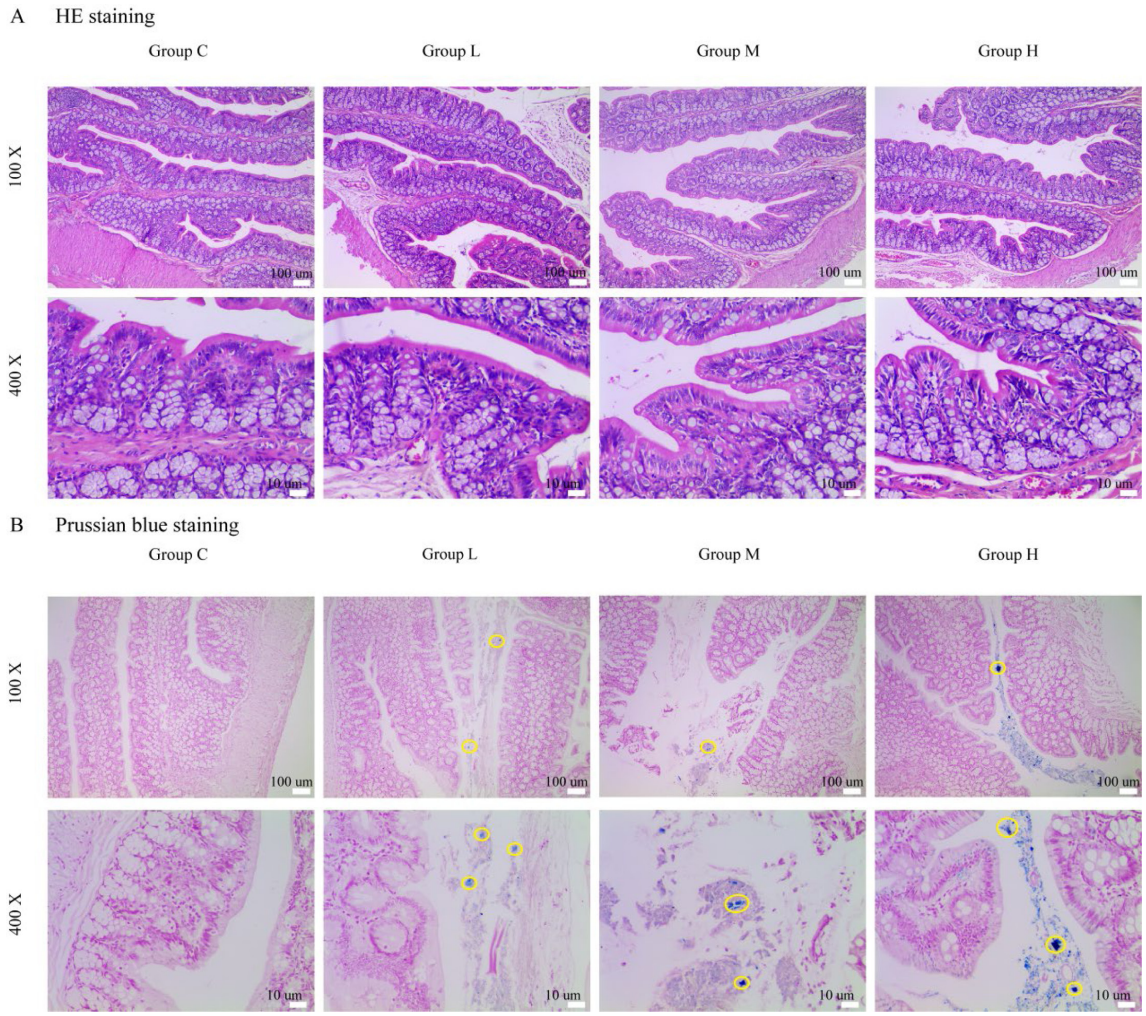

Fig. 1. HE staining (A) and Prussian blue staining (B) of cecal tissue (100× and 400×). The yellow circles are iron deposits in cecal tissues. HE: hematoxylin-eosin.

doi: 10.12938/bmfh.2023-012

34,152 sequences after quality control, with an average of 3,761 sequences per animal for those clustered at 97% sequence identity, and the Good's coverage index was 0.9758±0.0042. Moreover, the dilution curve flattened down as more extracted sequences were used (Supplementary Fig. 2), indicating an adequate depth of sequencing and that they could be used for further research. Alpha diversity was used to estimate the community richness (observed species and Chao 1 index) and diversity (Shannon index) of the gut microbiota. No statistically significant differences were found in either the cecal digesta or cecal mucosa between the control and IONP-treated groups (Fig. 2A–2C, 2E–2G). Principal coordinate analysis was conducted to differentiate the gut microbiota patterns in the cecal digesta and cecal mucosa of the different treated groups (Fig. 2D, 2H). The results for the cecal digesta and cecal mucosa did not differentiate the IONP treatment groups from the control group.

Effects of IONPs on the composition of gut microbiota

At the phylum level, the microbial compositions in the cecal digesta and cecal mucosa were obviously different (Fig. 3A), and Firmicutes, Bacteroidetes, and Proteobacteria were the predominant phyla in the cecal digesta and cecal mucosa. The bacterial taxonomic compositions of the cecal digesta in groups C, L, M, and H (CDC, CDL, CDM, and CDH, respectively) showed high relative abundances of *Firmicutes* (29.67%, 40.76%, 41.89%, and 46.10%), followed by *Bacteroidetes* (39.71%, 38.60%, 39.86%, and 37.39%), *Proteobacteria* (22.70%, 15.88%, 16.50%, and 10.71%), and *Actinobacteria* (4.12%, 2.64%, 4.32%, and 3.82%). Those of the cecal mucosa in groups C, L, M, and H (CMC, CML, CMM, and CMH, respectively) showed high relative abundances of *Proteobacteria* (33.33%, 32.63%, 30.40%, and 22.56%), followed by *Bacteroidetes* (21.46%, 21.50%, 22.94%, and 25.50%), *Firmicutes* (19.31%, 20.96%, 23.60%, and 34.40%), and *Actinobacteria* (12.08%, 11.61%, 10.95%, and 8.26%). A consistent finding between the cecal digesta and cecal mucosa was that high-dose IONPs increased the relative abundance of *Firmicutes* compared with the control group ($p<0.05$; Fig. 3B).

Specific bacterial taxa associated with IONP exposure

An LeFSe analysis was conducted to illustrate the effects of IONPs on the gut bacterial profile in rats at different phylogenetic levels (from phylum to species). At the phylum level, the relative abundances of Firmicutes were higher in the CDH and CMH, which was consistent with the results presented in Fig. 3B. Most of the specific bacterial taxa in cecal microbiota belonged to three dominant phyla: Firmicutes, Proteobacteria, and Actinobacteria.

At the genus level, the relative abundance of *Ruminococcaceae_UCG_014* was significantly increased in the CDM, CDH, and CMH (Fig. 4B–4E). Furthermore, the abundance of *Ruminiclostridium_9* was higher in the CDL (Fig. 4A, 4E), and the abundances of *Romboutsia* and *Bilophila* were markedly increased in the CDH (Fig. 4C, 4E). High-dose IONP exposure significantly increased the abundance of *Marvinbryantia* in the cecal mucosa; notably, *Bifidobacterium*, *Solanum_torvum*, and *Desulfovibrio* were significantly diminished in the CMH compared with the CMC (Fig. 4D, 4E). However, the genus levels in the CML and CMM were not significantly changed compared with the control group.

Effects of IONPs on gut microbial community function

According to the above effects of IONPs on intestinal microbial diversity and composition, more significant changes were found in the high-dose group. Therefore, the high-dose group was selected for the PICRUSt analysis to determine the functional changes of microbial communities. The KEGG categories indicated that functions related to energy metabolism, carbohydrate metabolism, lipid metabolism, amino acid metabolism, infectious diseases, the immune system, immune system diseases, and metabolic diseases (L2 level) and related to carbohydrate digestion and absorption,

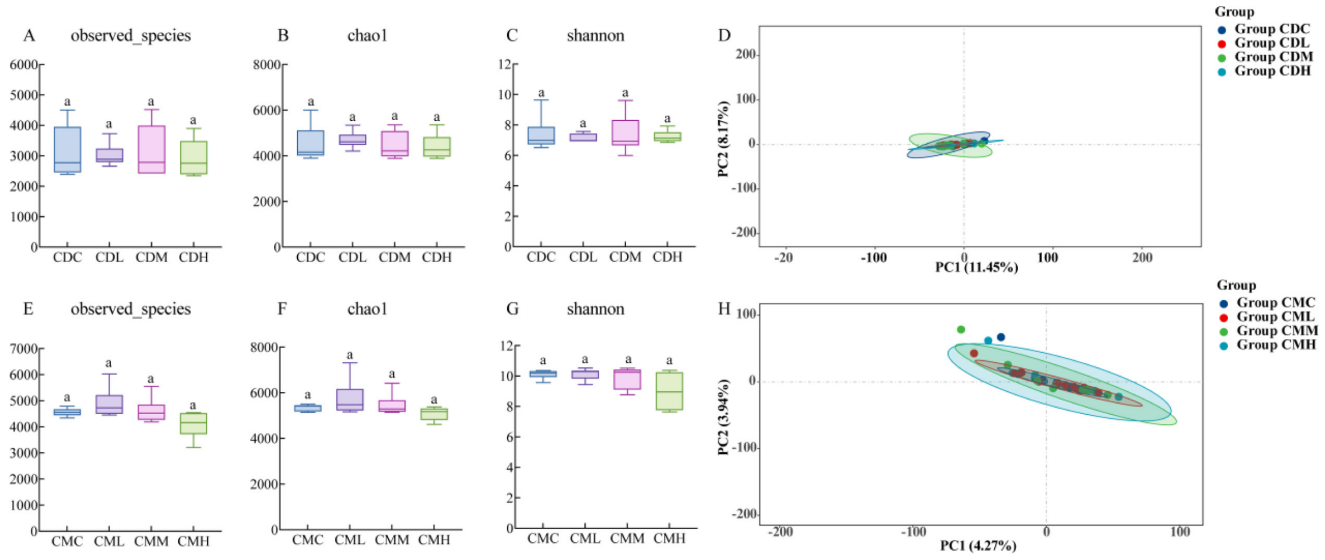

Fig. 2. Effects of IONPs on the α- and *β*-diversity of gut microbiota in the cecal digesta and cecal mucosa (n=6). Comparison by one-way ANOVA or Kruskal–Wallis H-test. Different lowercase letters indicate significant differences ($p<0.05$) in the diversity indices of the different groups (n=6). CDC: cecal digesta of the control group; CDL: cecal digesta of low-dose group; CDM: cecal digesta of medium dose group; CDH: cecal digesta of high-dose group; CMC: cecal mucosa of the control group; CML: cecal mucosa of low-dose group; CMM: cecal mucosa of medium-dose group; CMH: cecal mucosa of high-dose group; IONPs: iron(III) oxide nanoparticles; ANOVA: analysis of variance.

doi: 10.12938/bmfh.2023-012

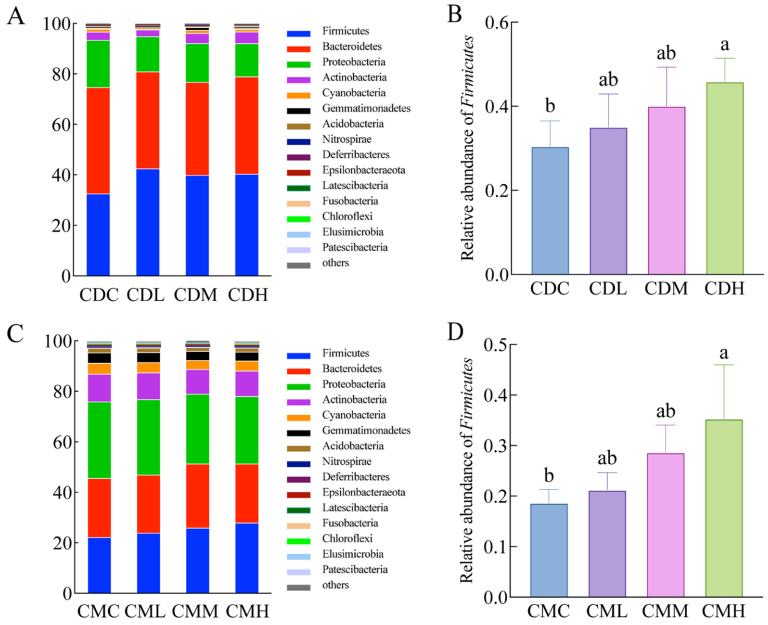

Fig. 3. Top 10 most abundant taxa of all samples at the phylum level in the cecal digesta (A) and cecal mucosa (C) and the relative abundances of Firmicutes in the cecal digesta (B) and cecal mucosa (D). Comparison by one-way ANOVA or Kruskal–Wallis H-test. Different lowercase letters indicate significant differences ($p<0.05$) in different groups (n=6). CDC: cecal digesta of the control group; CDL: cecal digesta of low-dose group; CDM: cecal digesta of medium dose group; CDH: cecal digesta of high-dose group; CMC: cecal mucosa of the control group; CML: cecal mucosa of low-dose group; CMM: cecal mucosa of medium-dose group; CMH: cecal mucosa of high-dose group; ANOVA: analysis of variance.

butanoate metabolism, arachidonic acid metabolism, tryptophan metabolism, bacterial toxins, Staphylococcus aureus infection, lipopolysaccharide biosynthesis, the insulin signaling pathway, and Type II diabetes mellitus (L3 level) were obviously affected in the cecal digesta and cecal mucosa after exposure to the high dose of IONPs (Fig. 5).

Effects of IONPs on the production of SCFAs in feces

The gut microbial and functional alterations prompted us to further confirm the impact of IONPs on SCFA levels. The changes in the concentrations of SCFAs in the four dosage groups and gavage times are shown in Fig. 6. As the exposure time increased, the IONPs showed evident influences on the rats. The concentrations of valeric acid, isobutyric acid, and isovaleric acid were significantly increased, though to different extents, compared with those in group C at 14 and 28 days of IONP exposure. The levels of acetic acid, butyric acid, and propionic acid also increased in groups L, M, and H compared with group C, but the differences were not significant (Fig. 6C, 6D).

Correlation analyses between the SCFAs and gut microbiota

Spearman's correlation coefficients were calculated to analyze the relationships between gut microbiota and metabolites. The top 30 gut microbiota at the genus level and the concentrations of SCFAs were visualized using a heatmap. *Ruminococcaceae_UCG-014*, *Romboutsia*, and *Bilophila*, which are IONP-enhanced bacteria in the cecal digesta (Fig. 4E), were positively correlated with the levels of isobutyric acid and isovaleric acid (Fig. 7A). In addition, *Ruminococcaceae_UCG-014* and *Marvinbryantia* exhibited positive correlations with the levels of butyric acid, valeric acid, isobutyric acid, and isovaleric acid in the cecal mucosa (Fig. 7B). Decreased abundances of *Desulfovibrio* and *Bifidobacterium* were associated with higher levels of isobutyric acid and isovaleric acid.

DISCUSSION

Fe is an essential element in the body required for various physiological functions, including oxygen transport and mitochondrial and DNA synthesis [28]. Therefore, IONPs were initially considered safe, biocompatible, biodegradable, and nontoxic materials [29], and some assays found that they were unlikely to have adverse effects [30]. However, there was evidence from *in vitro* and *in vivo* studies suggesting that IONPs could have harmful effects [31]. Additionally, iron is also extensively required across the domain of bacteria, as it functions as a co-factor in iron-containing proteins for redox reactions, metabolic pathways, and electron transport chain mechanisms, so bacteria can compete with the host for iron in order to survive and proliferate [32]. As an important part of the intestinal tract, the gut microbiota is closely related to the digestion and absorption of food, and disorders of the gut microbiota are associated with many diseases [33]. Intestinal bacteria consist of luminal and adherent bacteria [34], it has been recognized that intestinal mucosa-associated microbes are very different from the luminal microbiota [35]. Due to the close proximity of mucosa-associated microbiota to the host epithelium, intestinal mucosal-associated microbiota are more likely to impact the gut immune system and respond better to the connection between illness and health [36, 37], so exploring the changes both in digesta- and mucosa-associated microbes is meaningful. In this study, we illuminated how IONPs affect cecal digesta and mucosal microorganisms and their metabolites, SCFAs, in SD rats.

doi: 10.12938/bmfh.2023-012

The size of the IONPs used in our study was determined to be 70 ± 10 nm by TEM analysis, and the zeta potential was +25 mV at pH 7. We found that organ weights, biochemical indices, and cecal pathology were not obviously adversely damaged. These results were consistent with previous studies by Yun *et al.* [38], who administered IONPs (primary size, 60 nm) at 1,000 mg/kg, and Woo *et al.* [39], who administered IONPs (11.6 ± 0.7 nm) at 2 mg Fe/kg and 10 mg Fe/kg.

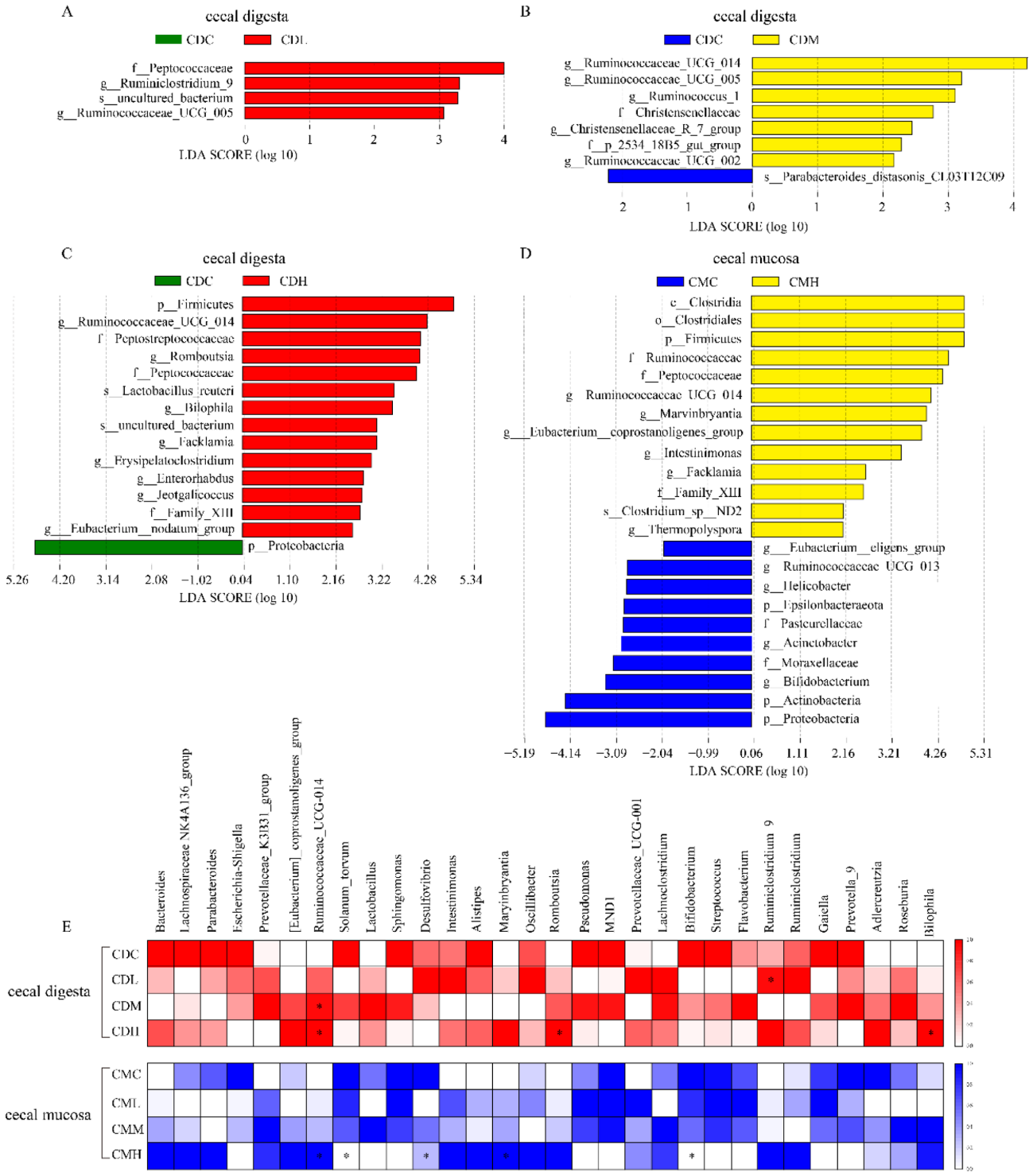

Fig. 4. Differences in gut microbiota abundance in the cecal digesta and cecal mucosa (n=6). (A) LDA for CDC vs. CDL; (B) LDA for CDC vs. CDM; (C) LDA for CDC vs. CDH; (D) LDA for CMC vs. CMH; (E) genera heatmap. Red indicates the top 30 genera of bacteria in the cecal digesta. Blue indicates the top 30 genera of bacteria in the cecal mucosa. Comparison by t-test or Mann–Whitney U test. *Significant difference vs. group C ($p<0.05$). LDA: linear discriminant analysis; CDC: cecal digesta of the control group; CDL: cecal digesta of low-dose group; CDM: cecal digesta of medium dose group; CDH: cecal digesta of high-dose group; CMC: cecal mucosa of the control group; CML: cecal mucosa of low-dose group; CMM: cecal mucosa of medium-dose group; CMH: cecal mucosa of high-dose group.

doi: 10.12938/bmfh.2023-012

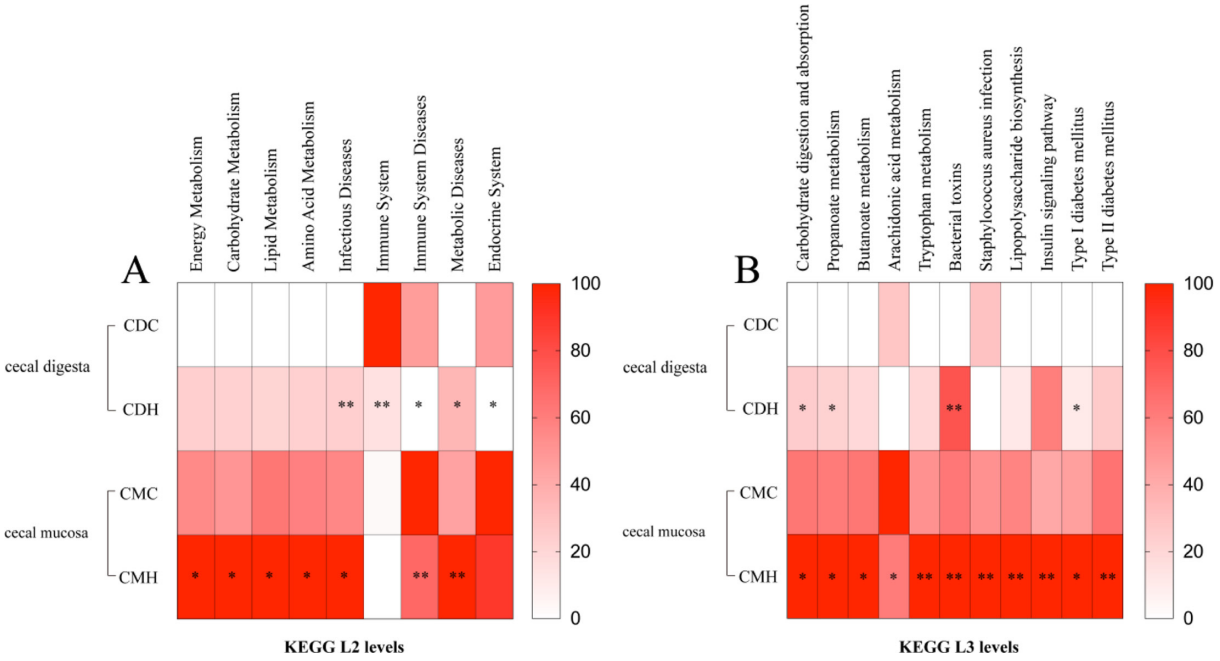

Fig. 5. Gut microbial communities of second-level (A) and third-level (B) metabolic pathways (n=6). Comparison by t-test or Mann–Whitney U test. *p<0.05 (high-dose group vs. control group); **p<0.01 (high-dose group vs. control group). CDC: cecal digesta of the control group; CDH: cecal digesta of high-dose group; CMC: cecal mucosa of the control group; CMH: cecal mucosa of high-dose group.

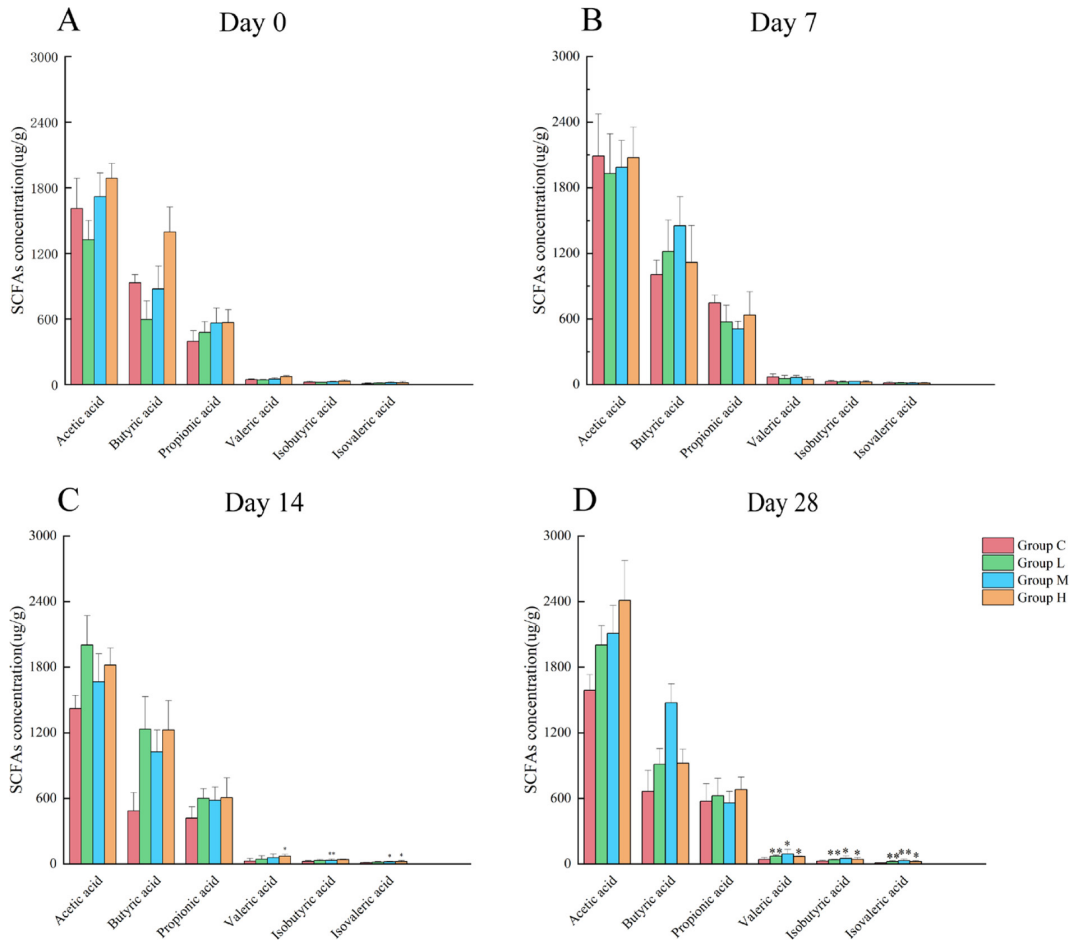

Fig. 6. SCFA concentrations in fecal samples on days 0 (A), 7 (B), 14 (C), and 28 (D; n=6). *p<0.05 (vs. group C); **p<0.01 (vs. group C). SCFA: short-chain fatty acid.

doi: 10.12938/bmfh.2023-012

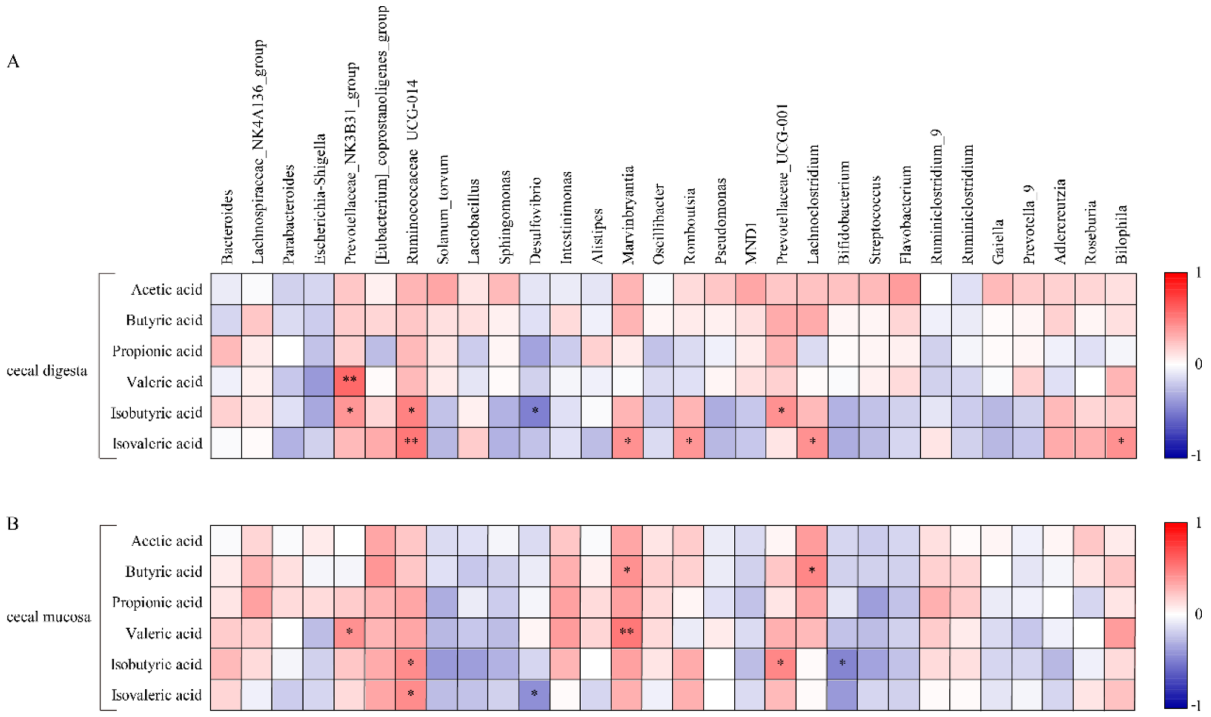

Fig. 7. Spearman's correlations between the gut microbiota and SCFAs in the cecal digesta (A) and cecal mucosa (B). *p<0.05; **p<0.01. SCFA: short-chain fatty acid.

Inorganic NPs are generally not digested in the GIT, but some may be partially or fully dissolved as a result of alterations in pH or dilution. Any NPs that are not absorbed or digested in the upper GIT will reach the lower GIT, where they may alter the microbiome [40]. In particular, our current results indicated that the rats treated with the low (50 mg/kg·bw), medium (100 mg/kg·bw), and high (200 mg/kg·bw) doses of IONPs for 28 days showed no significant effects on the α- and β-diversities of digesta- and mucosa-associated microbiota. Although there is currently no research on the impact of IONPs on intestinal microbes, it has been discovered from other literature that adding iron sulfate to mouse feed had no influence on the Shannon diversity index or total number of OTUs of cecal microbiota but induced significant compositional alterations [41], which is the same as our current findings.

Firmicutes, Bacteroidetes, Proteobacteria, and Actinobacteria comprise approximately 99% of the normal human gut microbiota [42], and Proteobacteria and Actinobacteria are the most abundant phyla of bacteria in the human- and mouse-associated mucosa [43]. Our study showed similar results. It has been proposed that Firmicutes are more effective in extracting energy from food than Bacteroidetes, thus promoting more efficient absorption of energy and subsequent weight gain [44, 45]. After treatment with 200 mg/kg IONPs, the body weights of rats and relative abundance of *Firmicutes* were increased, and the same results were observed in other iron-supplemented populations [46, 47] and mice [48]. Meanwhile, functional analysis of the gut microbiota indicated that oral iron affected metabolism function and increased a variety of metabolic processes pertaining to material metabolism, which could improve nutrition absorption and impact animal growth.

The relative abundances of *Ruminococcaceae_UCG-014*, *Ruminiclostridium_9*, *Romboutsia*, and *Bilophila* were increased by IONPs in the cecal digesta, and *Ruminococcaceae_UCG-014* displayed a dose-related trend. *Ruminococcaceae_UCG-014* and *Ruminiclostridium_9* belong to the *Ruminococcaceae*, and some bacteria in *Ruminococcaceae* are proinflammatory bacteria and associated with inflammatory bowel diseases [49, 50]. It has been shown that *Ruminococcaceae_UCG-014* and *Ruminiclostridium_9* are positively associated with proinflammatory cytokines and obesity [51, 52], and previous research has shown that *Ruminococcaceae_UCG-014* is positively correlated with the occurrence and development of diabetes [50, 53]. The relative abundance of *Romboutsia* in the intestine of patients with type I diabetes, ulcerative colitis, and rheumatoid arthritis is lower than that of healthy people [54] and is positively correlated with pro-inflammatory factors [55, 56]. Iron supplementation could lead to an increase in fecal calprotectin, which is thought to be a sign of increased intestinal inflammation [57]; even worse, oral iron can aggravate the inflammatory response in animals with colitis [32]. *Bilophila* is pathogenic bacteria [58], and research has revealed that *Romboutsia* and *Bilophila* are obesity-related bacteria [22, 59, 60]. Obesity is characterized by chronic, systemic, low-grade inflammation. IONPs have been proven to cause local and systemic inflammation and oxidative stress damage [61, 62], and an elevated luminal Fe concentration possibly results in the generation of ROS to increase inflammatory reactions [41, 63, 64], thereby disrupting glucose metabolism [65]. Our previous studies and this work have also found this [8], and IONPs not only increased body weight but also improved insulin-related metabolic functions. Therefore, we thought that IONP administration may contribute to the development of obesity and inflammation, further affecting endocrine and metabolic diseases such as diabetes.

doi: 10.12938/bmfh.2023-012

On the other hand, we found that only the high-dose IONP treatment increased the abundances of *Ruminococcaceae_UCG-014* and *Marvinbryantia* and decreased the abundances of *Bifidobacterium* in the cecal mucosa. This is probably because of the dilution of the host defense molecules in the external mucus layer, and the mucosa-associated microbiota was more stable than the luminal microorganisms [66]. Here we also saw that the relative abundance of *Ruminococcaceae_UCG-014* increased in the CMH, suggesting that there was a close relationship between the intake of IONPs and *Ruminococcaceae_UCG-014*. Zhang *et al.* [67] found that the abundance of *Ruminococcaceae_UCG-014* in pigs was negatively correlated with tissue iron levels, which is inconsistent with the present study; this may be due to the different study animals. *Bilophila* is a genus of lipopolysaccharide (LPS)-producing and mucosa-damaging bacteria [68], *Marvinbryantia* is a characteristic bacteria in the colonic mucosal microbiota [69], and *Bifidobacterium* can competitively occupy the surface of the intestinal mucosa, preventing the invasion of pathogenic bacteria and reducing the absorption of LPS [70]. Dietary iron supplementation could injure the intestine and induce higher levels of pathogenic gut bacteria [71], and it can also decrease the relative abundances of beneficial commensal bacteria such as *Bifidobacterium* species [72]. Many reports have demonstrated that excessive iron consumption reduces *Bifidobacterium* diversity [47, 57, 73] and raises LPS production [74] in animals and infants, affecting the immune system. Our KEGG functional predictions indicated that IONPs lead to enhanced functions related to infectious diseases, immune system diseases, bacterial toxins, *S. aureus* infection, and LPS biosynthesis, indicating that higher doses of IONPs may produce harmful bacteria that damage the cecal mucosa and negatively impact the immune system by causing the production of bacterial toxins.

Iron levels in the intestinal lumen can modify the microbiota composition and subsequently affect the microbiome's functionality in regards to its metabolomic profile, including SCFAs [71]. A previous study found that iron insufficiency caused SCFAs levels to drop but that iron supplementation raised them [75, 76], which is consistent with our results. This could be due to increased abundances of the Firmicutes phylum; *Ruminococcaceae_UCG-014* and *Ruminiclostridium_9* producing SCFAs, such as acetate and butyrate [77, 78]; and the SCFA metabolism-related pathways being enhanced. Organic acids produced by microbial fermentation could reduce the intestinal pH, thereby increasing the solubility of iron and promoting its absorption [32]. In addition, *Ruminococcaceae_UCG-014* is negatively correlated with intestinal motility, which strengthens the absorption of nutrients [79]. Therefore, we thought that another role for the increase in the Firmicutes phylum, *Ruminococcaceae_UCG-014,* and *Ruminiclostridium_9* was promotion of the absorption of iron in the body.

Unfortunately, we realized that our oral IONP trial suffered from some limitations. This included the fact that we did not investigate the fate of the IONPs in the GIT, which is determined by the physicochemical properties of the NPs, GIT fluids, surface-active components, and other factors [3]. Iron homeostasis in the host affects the makeup of the gut microbiota and the interaction between the host and gut microbiota through multiple pathways, including oxidative stress, nutrition homeostasis, intestinal permeability, and gut immunity [80], and the release of iron from IONPs can affect iron homeostasis and result in a series of changes, which comprises a complex and variable state. Therefore, the mechanisms by which IONPs interact with the intestinal microbiota and human health are interesting and worthy of further study.

In conclusion, our subacute repeated oral toxicity study indicated that IONPs increased the abundance of some harmful bacteria, elevated levels of SCFAs, and altered bacterial microbial energy metabolism, diabetes, bacterial infection, and immune-related functions. We also found that the microorganisms in the cecal digesta differed from those in the cecal mucosa, and only high-dose IONP (200 mg/kg) exposure changed the abundance and composition of mucosa-associated microbiota.

AUTHOR CONTRIBUTIONS

Shi Jiangchun and Li Yulin designed the study; Shi Jiangchun, Li Yulin, and Ren Dongxia carried out the experiments and conducted data collection; Shi Jiangchun, Xie Yumeng, Shao Huangfang, Liu Yang, and Wang Xue analyzed the data and discussion; Shi Jiangchun, Ren Dongxia, Zhang Yiqi, and Li Yun wrote and revised the manuscript. All authors have read and agreed to the published version of the manuscript.

CONFLICT OF INTEREST

The authors have no conflicts of interest to declare, and all have read and approved the manuscript and agreed to its submission. There are no other persons who satisfy the criteria for authorship.

REFERENCES

1. Lavorato GC, de Almeida AA, Vericat C, Fonticelli MH. 2023. Redox phase transformations in magnetite nanoparticles: impact on their composition, structure and biomedical applications. Nanotechnology 34: 1–27. [Medline] [CrossRef]
2. Scientific Opinion on the re-evaluation of iron oxides and hydroxides (E 172) as food additives. 2015. Science, safe food, sustainability (EFSA).
3. Yarjanli Z, Ghaedi K, Esmaeili A, Rahgozar S, Zarrabi A. 2017. Iron oxide nanoparticles may damage to the neural tissue through iron accumulation, oxidative stress, and protein aggregation. BMC Neurosci 18: 51. [Medline] [CrossRef]
4. Chrishtop VV, Mironov VA, Prilepskii AY, Nikonorova VG, Vinogradov VV. 2021. Organ-specific toxicity of magnetic iron oxide-based nanoparticles. Nanotoxicology 15: 167–204. [Medline] [CrossRef]
5. Patil US, Adireddy S, Jaiswal A, Mandava S, Lee BR, Chrisey DB. 2015. *In vitro*/*in vivo* toxicity evaluation and quantification of iron oxide nanoparticles. Int J Mol Sci 16: 24417–24450. [Medline] [CrossRef]
6. Liu Y. 2022. Biodistribution and excretion of iron oxide nanoparticles in rats after repeated oral exposure. Mod Prev Med 49: 3565–3571.
7. Shao HF, Liu Y, Wang X, Wang D, Ren DX, Li YL, Li Y. 2022. Immunotoxicity of subchronic oral exposure of iron oxide nanoparticles in rats. Wei Sheng Yen Chiu 51: 266–270.
8. Ren D, Li Y, Xue Y, Tang X, Yong L, Li Y. 2021. A study using LC-MS/MS-based metabolomics to investigate the effects of iron oxide nanoparticles on rat liver. NanoImpact 24: 100360. [Medline] [CrossRef]
9. Pereira DI, Aslam MF, Frazer DM, Schmidt A, Walton GE, McCartney AL, Gibson GR, Anderson GJ, Powell JJ. 2015. Dietary iron depletion at weaning imprints low microbiome diversity and this is not recovered with oral Nano Fe(III). MicrobiologyOpen 4: 12–27. [Medline] [CrossRef]
10. Xie JN, Zhao MR, Wang CY, Yong Y, Gu Z. 2022. Recent advances in understanding the effects of nanomaterials on gut microbiota. Chem Eng J 435: 134976. [CrossRef]
11. Chen J, Zhang S, Chen C, Jiang X, Qiu J, Qiu Y, Zhang Y, Wang T, Qin X, Zou Z, Chen C. 2020. Crosstalk of gut microbiota and serum/hippocampus metabolites in neurobehavioral impairments induced by zinc oxide nanoparticles. Nanoscale 12: 21429–21439. [Medline] [CrossRef]
12. Pereira DI, Bruggraber SF, Faria N, Poots LK, Tagmount MA, Aslam MF, Frazer DM, Vulpe CD, Anderson GJ, Powell JJ. 2014. Nanoparticulate iron(III) oxo-hydroxide delivers safe iron that is well absorbed and utilised in humans. Nanomedicine 10: 1877–1886. [Medline] [CrossRef]
13. Qiu KY, Durham PG, Anselmo AC. 2018. Inorganic nanoparticles and the microbiome. Nano Res 11: 4936–4954. [CrossRef]

14. Medina-Reyes EI, Rodríguez-Ibarra C, Déciga-Alcaraz A, Díaz-Urbina D, Chirino YI, Pedraza-Chaverri J. 2020. Food additives containing nanoparticles induce gastrotoxicity, hepatotoxicity and alterations in animal behavior: the unknown role of oxidative stress. Food Chem Toxicol 146: 111814. [Medline] [CrossRef]
15. Suriano F, Nyström EEL, Sergi D, Gustafsson JK. 2022. Diet, microbiota, and the mucus layer: the guardians of our health. Front Immunol 13: 953196. [Medline] [CrossRef]
16. Chen M, Lin W, Li N, Wang Q, Zhu S, Zeng A, Song L. 2022. Therapeutic approaches to colorectal cancer *via* strategies based on modulation of gut microbiota. Front Microbiol 13: 945533. [Medline] [CrossRef]
17. Zhang P. 2022. Influence of foods and nutrition on the gut microbiome and implications for intestinal health. Int J Mol Sci 23: 9588. [Medline] [CrossRef]
18. Melo NCO, Cuevas-Sierra A, Fernández-Cruz E, de la O V, Martínez JA. 2023. Fecal microbiota composition as a metagenomic biomarker of dietary intake. Int J Mol Sci 24: 4918. [Medline] [CrossRef]
19. Valder S, Brinkmann C. 2022. Exercise for the diabetic gut-potential health effects and underlying mechanisms. Nutrients 14: 813. [Medline] [CrossRef]
20. Fan Y, Pedersen O. 2021. Gut microbiota in human metabolic health and disease. Nat Rev Microbiol 19: 55–71. [Medline] [CrossRef]
21. Cummings JH, Pomare EW, Branch WJ, Naylor CP, Macfarlane GT. 1987. Short chain fatty acids in human large intestine, portal, hepatic and venous blood. Gut 28: 1221–1227. [Medline] [CrossRef]
22. Hu S, Xu Y, Gao X, Li S, Jiang W, Liu Y, Su L, Yang H. 2019. Long-chain bases from sea cucumber alleviate obesity by modulating gut microbiota. Mar Drugs 17: 455. [Medline] [CrossRef]
23. Gajardo K, Rodiles A, Kortner TM, Krogdahl Å, Bakke AM, Merrifield DL, Sørum H. 2016. A high-resolution map of the gut microbiota in Atlantic salmon (*Salmo salar*): a basis for comparative gut microbial research. Sci Rep 6: 30893. [Medline] [CrossRef]
24. Bolger AM, Lohse M, Usadel B. 2014. Trimmomatic: a flexible trimmer for Illumina sequence data. Bioinformatics 30: 2114–2120. [Medline] [CrossRef]
25. Caporaso JG, Kuczynski J, Stombaugh J, Bittinger K, Bushman FD, Costello EK, Fierer N, Peña AG, Goodrich JK, Gordon JI, Huttley GA, Kelley ST, Knights D, Koenig JE, Ley RE, Lozupone CA, McDonald D, Muegge BD, Pirrung M, Reeder J, Sevinsky JR, Turnbaugh PJ, Walters WA, Widmann J, Yatsunenko T, Zaneveld J, Knight R. 2010. QIIME allows analysis of high-throughput community sequencing data. Nat Methods 7: 335–336. [Medline] [CrossRef]
26. Rognes T, Flouri T, Nichols B, Quince C, Mahé F. 2016. VSEARCH: a versatile open source tool for metagenomics. PeerJ 4: e2584. [Medline] [CrossRef]
27. Wang Q, Garrity GM, Tiedje JM, Cole JR. 2007. Naive Bayesian classifier for rapid assignment of rRNA sequences into the new bacterial taxonomy. Appl Environ Microbiol 73: 5261–5267. [Medline] [CrossRef]
28. Wang F, Wang J, Shen Y, Li H, Rausch WD, Huang X. 2022. Iron dyshomeostasis and ferroptosis: a new Alzheimer's disease hypothesis? Front Aging Neurosci 14: 830569. [Medline] [CrossRef]
29. Jeon M, Halbert MV, Stephen ZR, Zhang M. 2021. Iron oxide nanoparticles as T_1 contrast agents for magnetic resonance imaging: fundamentals, challenges, applications, and prospectives. Adv Mater 33: e1906539. [Medline] [CrossRef]
30. Sadiq R, Khan QM, Mobeen A, Shah A. 2021. Genotoxicity of aluminium oxide, iron oxide, and copper nanoparticles in mouse bone marrow cells. Arh Hig Rada Toksikol 72: 315–325. [Medline]
31. Abakumov MA, Semkina AS, Skorikov AS, Vishnevskiy DA, Ivanova AV, Mironova E, Davydova GA, Majouga AG, Chekhonin VP. 2018. Toxicity of iron oxide nanoparticles: size and coating effects. J Biochem Mol Toxicol 32: e22225. [Medline] [CrossRef]
32. Yilmaz B, Li H. 2018. Gut microbiota and iron: the crucial actors in health and disease. Pharmaceuticals (Basel) 11.
33. Jia B, Lin H, Yu S, Liu N, Yu D, Wu A. 2023. Mycotoxin deoxynivalenol-induced intestinal flora disorders, dysfunction and organ damage in broilers and pigs. J Hazard Mater 451: 131172. [Medline] [CrossRef]
34. Ma N, Ma X. 2019. Dietary amino acids and the gut-microbiome-immune axis: physiological metabolism and therapeutic prospects. Compr Rev Food Sci Food Saf 18: 221–242. [Medline] [CrossRef]
35. Ringel Y, Maharshak N, Ringel-Kulka T, Wolber EA, Sartor RB, Carroll IM. 2015. High throughput sequencing reveals distinct microbial populations within the mucosal and luminal niches in healthy individuals. Gut Microbes 6: 173–181. [Medline] [CrossRef]
36. Li Q, Wang C, Tang C, Li N, Li J. 2012. Molecular-phylogenetic characterization of the microbiota in ulcerated and non-ulcerated regions in the patients with Crohn's disease. PLoS One 7: e34939. [Medline] [CrossRef]
37. Gevers D, Kugathasan S, Denson LA, Vázquez-Baeza Y, Van Treuren W, Ren B, Schwager E, Knights D, Song SJ, Yassour M, Morgan XC, Kostic AD, Luo C, González A, McDonald D, Haberman Y, Walters T, Baker S, Rosh J, Stephens M, Heyman M, Markowitz J, Baldassano R, Griffiths A, Sylvester F, Mack D, Kim S, Crandall W, Hyams J, Huttenhower C, Knight R, Xavier RJ. 2014. The treatment-naive microbiome in new-onset Crohn's disease. Cell Host Microbe 15: 382–392. [Medline] [CrossRef]
38. Yun JW, Kim SH, You JR, Kim WH, Jang JJ, Min SK, Kim HC, Chung DH, Jeong J, Kang BC, Che JH. 2015. Comparative toxicity of silicon dioxide, silver and iron oxide nanoparticles after repeated oral administration to rats. J Appl Toxicol 35: 681–693. [Medline] [CrossRef]
39. Woo S, Kim S, Kim H, Cheon YW, Yoon S, Oh JH, Park J. 2021. Charge-modulated synthesis of highly stable iron oxide nanoparticles for *in vitro* and *in vivo* toxicity evaluation. Nanomaterials (Basel) 11: 3068. [Medline] [CrossRef]
40. Gupta A, Eral HB, Hatton TA, Doyle PS. 2016. Nanoemulsions: formation, properties and applications. Soft Matter 12: 2826–2841. [Medline] [CrossRef]
41. Werner T, Wagner SJ, Martínez I, Walter J, Chang JS, Clavel T, Kisling S, Schuemann K, Haller D. 2011. Depletion of luminal iron alters the gut microbiota and prevents Crohn's disease-like ileitis. Gut 60: 325–333. [Medline] [CrossRef]
42. Kim YS, Ho SB. 2010. Intestinal goblet cells and mucins in health and disease: recent insights and progress. Curr Gastroenterol Rep 12: 319–330. [Medline] [CrossRef]
43. ANCE N. 2007. Developments in anti-doping in elite sport. J Exerc Sci Fit 5: 75–78.
44. Liu Z, Zhou X, Wang W, Gu L, Hu C, Sun H, Xu C, Hou J, Jiang Z. 2022. *Lactobacillus paracasei* 24 attenuates lipid accumulation in high-fat diet-induced obese mice by regulating the gut microbiota. J Agric Food Chem 70: 4631–4643. [Medline] [CrossRef]
45. Krajmalnik-Brown R, Ilhan ZE, Kang DW, DiBaise JK. 2012. Effects of gut microbes on nutrient absorption and energy regulation. Nutr Clin Pract 27: 201–214. [Medline] [CrossRef]
46. Tang M, Frank DN, Sherlock L, Ir D, Robertson CE, Krebs NF. 2016. Effect of vitamin E with therapeutic iron supplementation on iron repletion and gut microbiome in US iron deficient infants and toddlers. J Pediatr Gastroenterol Nutr 63: 379–385. [Medline] [CrossRef]
47. Tang M, Frank DN, Hendricks AE, Ir D, Esamai F, Liechty E, Hambidge KM, Krebs NF. 2017. Iron in micronutrient powder promotes an unfavorable gut microbiota in Kenyan infants. Nutrients 9: 776. [Medline] [CrossRef]
48. Kortman GAM, Mulder MLM, Richters TJW, Shanmugam NKN, Trebicka E, Boekhorst J, Timmerman HM, Roelofs R, Wiegerinck ET, Laarakkers CM, Swinkels DW, Bolhuis A, Cherayil BJ, Tjalsma H. 2015. Low dietary iron intake restrains the intestinal inflammatory response and pathology of enteric infection by food-borne bacterial pathogens. Eur J Immunol 45: 2553–2567. [Medline] [CrossRef]
49. Liu R, Shu Y, Qi WH, Rao WL, Fu ZH, Shi ZX, Zhang ZS. 2021. Protective effects of almond oil on streptozotocin-induced diabetic rats via regulating Nrf2/HO-1 pathway and gut microbiota. J Food Qual 14: 5599219.
50. He S, Peng WB, Zhou HL, Fu XJ, Sun YH, Wang ZG. 2023. A combination of deep-sea water and fucoidan alleviates T2DM through modulation of gut microbiota and metabolic pathways. Pharmaceuticals (Basel) 16: 462. [Medline] [CrossRef]
51. Zhou Y, Zhang M, Liu Q, Feng J. 2021. The alterations of tracheal microbiota and inflammation caused by different levels of ammonia exposure in broiler chickens. Poult Sci 100: 685–696. [Medline] [CrossRef]
52. Li C, Cui L, Wang X, Yan Z, Wang S, Zheng Y. 2020. Using intestinal flora to distinguish non-alcoholic steatohepatitis from non-alcoholic fatty liver. J Int Med Res 48: 300060520978122. [Medline] [CrossRef]
53. Ma Q, Li Y, Wang J, Li P, Duan Y, Dai H, An Y, Cheng L, Wang T, Wang C, Wang T, Zhao B. 2020. Investigation of gut microbiome changes in type 1 diabetic mellitus rats based on high-throughput sequencing. Biomed Pharmacother 124: 109873. [Medline] [CrossRef]
54. Li P, Gao M, Song B, Yan S, Zhao Y, Gong L, Liu Y, Lv Z, Guo Y. 2022. Soya saponin fails to improve the antioxidation and immune function of laying hens with antibiotics treated. Poult Sci 101: 101921. [Medline] [CrossRef]
55. Cong S, Wang L, Meng Y, Cai X, Zhang C, Gu Y, Ma X, Luo L. 2023. Saussurea involucrata oral liquid regulates gut microbiota and serum metabolism during alleviation of collagen-induced arthritis in rats. Phytother Res 37: 1242–1259. [Medline] [CrossRef]
56. Wang HG, Zhang MN, Wen X, He L, Zhang MH, Zhang JL, Yang XZ. 2022. Cepharanthine ameliorates dextran sulphate sodium-induced colitis through modulating gut microbiota. Microb Biotechnol 15: 2208–2222. [Medline] [CrossRef]
57. Jaeggi T, Kortman GAM, Moretti D, Chassard C, Holding P, Dostal A, Boekhorst J, Timmerman HM, Swinkels DW, Tjalsma H, Njenga J, Mwangi A, Kvalsvig J, Lacroix C, Zimmermann MB. 2015. Iron fortification adversely affects the gut microbiome, increases pathogen abundance and induces intestinal inflammation in Kenyan infants. Gut 64: 731–742. [Medline] [CrossRef]
58. Xiao Y, Yang CM, Xu HJ, Wu QG, Zhou YM, Zhou XL, Miao JL. 2020. Procyanidin B2 prevents dyslipidemia via modulation of gut microbiome and related metabolites in high-fat diet fed mice. J Funct Foods 75: 104285. [CrossRef]
59. Yin H, Huang J, Guo X, Xia J, Hu M. 2023. *Romboutsia lituseburensis* JCM1404 supplementation ameliorated endothelial function via gut microbiota modulation and lipid metabolisms alterations in obese rats. FEMS Microbiol Lett 370: 1–9. [Medline] [CrossRef]
60. Pan LY, Zhou YY, Zhang X, Jiang HY. 2022. Gut microbiota is associated with weight gain in children treated with atypical antipsychotic: a pilot longitudinal study. Psychiatry Res 316: 114784. [Medline] [CrossRef]
61. Ramírez-Cando LJ, De Simone U, Coccini T. 2017. Toxicity evaluation of iron oxide (Fe_3O_4) nanoparticles on human neuroblastoma-derived SH-SY5Y cell line. J Nanosci Nanotechnol 17: 203–211. [Medline] [CrossRef]

62. Yu Q, Xiong XQ, Zhao L, Xu TT, Bi H, Fu R, Wang QH. 2018. Biodistribution and toxicity assessment of superparamagnetic iron oxide nanoparticles *in vitro* and *in vivo*. Curr Med Sci 38: 1096–1102. [Medline] [CrossRef]
63. Dostal A, Lacroix C, Pham VT, Zimmermann MB, Del'homme C, Bernalier-Donadille A, Chassard C. 2014. Iron supplementation promotes gut microbiota metabolic activity but not colitis markers in human gut microbiota-associated rats. Br J Nutr 111: 2135–2145. [Medline] [CrossRef]
64. Sriwichaiin S, Thiennimitr P, Thonusin C, Sarichai P, Buddhasiri S, Kumfu S, Nawara W, Kittichotirat W, Fucharoen S, Chattipakorn N, Chattipakorn SC. 2022. Deferiprone has less benefits on gut microbiota and metabolites in high iron-diet induced iron overload thalassemic mice than in iron overload wild-type mice: a preclinical study. Life Sci 307: 120871. [Medline] [CrossRef]
65. Zhang Z, Funcke JB, Zi Z, Zhao S, Straub LG, Zhu Y, Zhu Q, Crewe C, An YA, Chen S, Li N, Wang MY, Ghaben AL, Lee C, Gautron L, Engelking LJ, Raj P, Deng Y, Gordillo R, Kusminski CM, Scherer PE. 2021. Adipocyte iron levels impinge on a fat-gut crosstalk to regulate intestinal lipid absorption and mediate protection from obesity. Cell Metab 33: 1624–1639.e9. [Medline] [CrossRef]
66. Van den Abbeele P, Van de Wiele T, Verstraete W, Possemiers S. 2011. The host selects mucosal and luminal associations of coevolved gut microorganisms: a novel concept. FEMS Microbiol Rev 35: 681–704. [Medline] [CrossRef]
67. Zhang XL, Zhou YR, Xu SS, Xu S, Xiong YJ, Xu K, Xu CJ, Che JJ, Huang L, Liu ZG, Wang BY, Mu YL, Xiao SB, Li K. 2023. Characterization of gut microbiota compositions along the intestinal tract in *CD163/pAPN* double knockout piglets and their potential roles in iron aabsorption. Microbiol Spectr 11: e0190622. [Medline] [CrossRef]
68. Song JJ, Tian WJ, Kwok LY, Wang YL, Shang YN, Menghe B, Wang JG. 2017. Effects of microencapsulated *Lactobacillus plantarum* LIP-1 on the gut microbiota of hyperlipidaemic rats. Br J Nutr 118: 481–492. [Medline] [CrossRef]
69. Wu M, Li P, Li J, An Y, Wang M, Zhong G. 2020. The differences between luminal microbiota and mucosal microbiota in mice. J Microbiol Biotechnol 30: 287–295. [Medline] [CrossRef]
70. Ling X, Linglong P, Weixia D, Hong W. 2016. Protective effects of *Bifidobacterium* on intestinal barrier function in LPS-induced enterocyte barrier injury of caco-2 monolayers and in a rat NEC model. PLoS One 11: e0161635. [Medline] [CrossRef]
71. Botta A, Barra NG, Lam NH, Chow S, Pantopoulos K, Schertzer JD, Sweeney G. 2021. Iron reshapes the gut microbiome and host metabolism. J Lipid Atheroscler 10: 160–183. [Medline] [CrossRef]
72. Mayneris-Perxachs J, Moreno-Navarrete JM, Fernández-Real JM. 2022. The role of iron in host-microbiota crosstalk and its effects on systemic glucose metabolism. Nat Rev Endocrinol 18: 683–698. [Medline] [CrossRef]
73. Huynh U, Zastrow ML. 2023. Metallobiology of Lactobacillaceae in the gut microbiome. J Inorg Biochem 238: 112023. [Medline] [CrossRef]
74. Ghadimi D, Yoness Hassan MF, Fölster-Holst R, Röcken C, Ebsen M, de Vrese M, Heller KJ. 2020. Regulation of hepcidin/iron-signalling pathway interactions by commensal bifidobateria plays an important role for the inhibition of metaflammation-related biomarkers. Immunobiology 225: 151874. [Medline] [CrossRef]
75. Dostal A, Chassard C, Hilty FM, Zimmermann MB, Jaeggi T, Rossi S, Lacroix C. 2012. Iron depletion and repletion with ferrous sulfate or electrolytic iron modifies the composition and metabolic activity of the gut microbiota in rats. J Nutr 142: 271–277. [Medline] [CrossRef]
76. Paganini D, Zimmermann MB. 2017. The effects of iron fortification and supplementation on the gut microbiome and diarrhea in infants and children: a review. Am J Clin Nutr 106 Suppl 6: 1688S–1693S. [Medline] [CrossRef]
77. Tian B, Zhao J, Zhang M, Chen Z, Ma Q, Liu H, Nie C, Zhang Z, An W, Li J. 2021. *Lycium ruthenicum* anthocyanins attenuate high-fat diet-induced colonic barrier dysfunction and inflammation in mice by modulating the gut microbiota. Mol Nutr Food Res 65: e2000745. [Medline] [CrossRef]
78. Qu L, Ren J, Huang L, Pang B, Liu X, Liu X, Li B, Shan Y. 2018. Antidiabetic effects of *Lactobacillus casei* fermented yogurt through reshaping gut microbiota structure in type 2 diabetic rats. J Agric Food Chem 66: 12696–12705. [Medline] [CrossRef]
79. Chai M, Wang L, Li X, Zhao J, Zhang H, Wang G, Chen W. 2021. Different *Bifidobacterium bifidum* strains change the intestinal flora composition of mice *via* different mechanisms to alleviate loperamide-induced constipation. Food Funct 12: 6058–6069. [Medline] [CrossRef]
80. Xiao L, Tang R, Wang J, Wan D, Yin Y, Xie L. 2023. Gut microbiota bridges the iron homeostasis and host health. Sci China Life Sci 66: 1952–1975. [Medline] [CrossRef]

